# Measuring capture, internalization and cytosolic delivery of extracellular vesicle-embedded syntenin

Lukas Hyka[(1)], Eliane Jaafar[(1)], Sofie Meeussen[(1)], Alain Joliot[(3)] , Guido David[(1,2)] and Pascale Zimmermann[(1,2)*]

[1]Laboratory for Extracellular Vesicle Research, Department of Human Genetics, Katholieke Universiteit Leuven, Leuven, Belgium

[2]Centre de Recherche en Cancérologie de Marseille (CRCM), Equipe Labellisée Ligue 2018, CNRS, Inserm, Institut Paoli Calmettes, Aix-Marseille Université, Marseille, France.

[3]INSERM U932, Institut Curie Centre de Recherche, PSL Research University, Paris, France.

*** Corresponding author:** Pascale Zimmermann (Pascale.Zimmermann@kuleuven.be).

**Abstract**

Extracellular vesicles (EVs) mediate cell-to-cell communication and are considered potential drug delivery vehicles. Nevertheless, whether EV-embedded cargo can be efficiently delivered into the cytosol of recipient cells remains debated. Here, we investigated the fate of syntenin, a well-established internal cargo of small EVs (sEVs).

Using quantitative assays, we show that ~85% of internalized sEV-embedded syntenin can be delivered to the cytosol of recipient cells within short periods of time. Yet, even at low dose, we find that the internalization of sEVs carrying syntenin is rather inefficient (~0.03% of the administered dose). Moreover, we observe that the capture of sEVs by recipient cells is non-saturable over time and largely more efficient than their internalization. Finally, we identify the N-terminal domain of syntenin and the phosphorylation state of a Src-targeted tyrosine residue in this domain, as key determinants for its incorporation into sEVs that support cytosolic delivery.

These findings challenge, current views in the field by indicating that sEV internalization may be a marginal process (on the contrary to capture) and that cytosolic delivery can be highly efficient. Moreover, our study identifies molecular determinants governing cytosolic delivery of sEV-embedded syntenin.

**Key words:** EV capture, EV internalization, EV cargo delivery, quantitative assays, syntenin.

## Introduction

Extracellular vesicles (EVs) are membrane-limited organelles released and taken up by all cell types. What remains a matter of debate is whether EV embedded or inner cargo can be efficiently delivered into the cytosol of EV recipient cells[1].

Syntenin is a member of the PDZ domain-containing scaffold protein family that is involved in multiple cellular processes, including cell adhesion[2], transcriptional activation[3], and cell growth, proliferation, and cell cycle progression[4]. Importantly, using structure-function approaches, we established that syntenin is a key organizer of small extracellular vesicle (sEV) biogenesis, affecting up to 50% of the sEV population in the extracellular space[5–7].

Structurally, syntenin consists of four domains: N-terminal domain, two central PDZ domains (PDZ1 and PDZ2), and a C-terminal domain, each mediating specific molecular interactions. In particular, the N-terminal domain of syntenin binds Alix via three repeats of the LYPXL motif (reminiscent of late viral domains implicated in viral budding). Together with Alix and syndecans, syntenin functions as a key component of sEV biogenesis by stimulating intraluminal vesicle accumulation in multivesicular bodies that support the secretion of sEVs[5]. Furthermore, the small GTPase ARF6 and its effector phospholipase D2 support this sEV biogenesis pathway, and the PDZ1 domain of syntenin binds the fusogenic lipid phosphatidic acid, the product of PLD2 activity[8]. Syndecans are abundant transmembrane proteins carrying heparan sulfate that strongly interact with the PDZ2 domain of syntenin and that support sEV biology in various manners[5,9,10]. In particular, we found that and syntenin support sEV-mediated pro-migratory activities upon phosphorylation of specific tyrosine residue by Src kinase in sEV producing cells[11].

Despite the important role of syntenin in sEV biology and also its high abundance in these organelles [5,12], the fate of sEV-embedded syntenin, including its delivery into the cytosol of recipient cells, remains uninvestigated. Here, we use fluorescence and bioluminescence complementation assays to determine how efficiently sEV-embedded syntenin can be captured, internalized, and delivered into the cytosol of recipient cells. Moreover, we define molecular determinants that control cytosolic delivery of sEV-embedded syntenin.

## Materials and methods

## Reagents & antibodies

Fetal bovine serum (FBS, Sigma, 1681067), DMEM (Gibco, 41965039), XtremeGene 9 (Roche, 6365809001), Geneticin (Gibco, 10131027), EV-depleted FBS (FBS depleted of intrinsic EVs by overnight (18 h) centrifugation at 100,000 x g, followed by filtration through sterile 0.45 µm filters (Merck), Amicon 10 kDa filters (Merck, UFC901024), Furimazine (DC chemicals, DC70371). Cell mask deep red (ThermoFisher, C10046) staining was used according to the manufacturer's instructions. The syntenin-1 antibody is homemade and was described before[2]. The antibodies against CD9, CD63 were kind gifts of Prof. Eric Rubinstein[13] (Université Paris-Sud, Inserm UMRS 935, Villejuif, France). The anti-GFP antibody (Invitrogen, A11122) was used according to the manufacturer's instructions. In house purified rabbit anti-LgBiT antibody obtained by immunization of full-length Nanoluciferase (NL) was provided by Alain Joliot and Clotilde Thery (INSERM U932, Institut Curie Centre de Recherche, PSL Research University, Paris, France).

Plasmids encoding NL and its split fragments (HiBiT and LgBiT) were kindly provided by Alain Joliot. The HiBiT fragment was fused to syntenin and CD63 by overlapping PCR and Gateway recombination cloning. GFP split fragments were kindly provided by Stephanie Cabantous (CRCT, Toulouse). All the fusions of different tags to syntenin and CD63 were N-terminal. All open reading frames were verified by sequencing.

## Cell culture and transfections

HEK293, and MCF-7 cells (ATCC) were cultured in DMEM supplemented with 10% FBS. For transfections, HEK293 cells were plated the day before so to achieve ~40% confluency at the time of transfection. Cells were transfected with expression vectors using XtremeGene 9 according to the manufacturer's protocol. Following transfection, cells were cultured for 48 hours, washed once with fresh culture medium (DMEM) before microscopy or secretome collections.

## Preparation of stable clones

Expression vectors were linearized. After 48 hours of transfection, MCF-7 cells were put under Geneticin selection at 500 µg/ml. These concentrations were determined as the minimal doses inducing full cell death after 14 days. Resistant colonies were picked after 21 days and expanded separately. Transgene expression in total cellular

113 population was confirmed by confocal microscopy after immunostaining with anti-GFP
114 or anti-LgBiT antibody.

115 **Preparation of EVs by differential ultracentrifugation (dUC)**

116 For secretome collections cells were cultured in serum-free DMEM for 16 hours (5 ml
117 medium per 10 cm plate of 1.2 million cells (plated on day 1)). Conditioned media were
118 collected after 16 hours and subjected to three sequential centrifugation steps at 4°C:
119 10 min at 1,500 x g (50 ml Falcon tube, rotor Sigma 12310), to remove cells and cell
120 debris; 30 min at 10,000 x g (10K; 50 ml Falcon tube, rotor Sigma 12310) to pellet large
121 particles (lEVs); and 1 h at 100,000 x g (100K; Beckman Open-Top Thinwall Ultra-clear
122 Tube rotor SW32Ti) to pellet small particles (sEVs). 100K pellets were washed in PBS,
123 centrifugated for 1 h at 100,000 x g (Beckman Microfuge Tube Polyallomer, rotor TLA-
124 55), and re-suspended in 40 µl of PBS, as were 10K pellets for further analysis by
125 Western blot. The corresponding cell layers were kept on ice, scraped in lysis buffer
126 (Tris-HCl 25 mM, pH 7.4, NaCl 150 mM, EDTA 1 mM, NP40 1% and protease
127 inhibitors), and incubated for 45 min at 4°C under gentle agitation. Cell lysates were
128 cleared by centrifugation at 10, 000 x g at 4°C for 10 min before analysis by Western
129 blot.

130 **Preparation of EVs by concentrating conditioned medium (CCM sEVs)**

131 For secretome collections, cells were cultured in serum-free DMEM for 16 hours (5 ml
132 medium per 10 cm plate of 1.2 million cells (plated on day 1)). Conditioned media were
133 collected and processed as for dUC, for cell debris and lEVs removal. The 10K pellet
134 supernatant was loaded on Amicon 10 kDa filters and concentrated by centrifugation
135 at 2,000 x g until the volume dropped from ~10 ml to ~300 µl (33 x concentration). This
136 concentrated supernatant was referred to as the CCM sEV fraction and characterized
137 by Western blot or used in cell incubation experiments. For the comparison of GFP11
138 sorting with dUC (Fig. 1c, Supplementary Fig. 2) conditioned media were pooled upon
139 collection and then again separated. sEVs were then prepared as described in dUC or
140 CCM sEVs preparation sections.

141 **Immunofluorescence analyses**

142 The cells were cultured on eight-well chamber slides (Nalgene Nunc, 177402)
143 overnight, fixed with 4% PFA for 15 min, washed with PBS, and permeabilized with

144 0.05% saponin in PBS for 20 min, in the presence of 0.3% BSA for blocking non-
145 specific reactions. After incubation with primary antibodies, cells were incubated with
146 Alexa-conjugated secondary antibodies (Invitrogen). Cells were visualized either by
147 nuclei DAPI staining or by cell membrane staining using Cell mask deep red followed
148 by mounting with ProLong Glass Antifade Mountant (ThermoFisher, P36982). Samples
149 were observed with an Olympus Fluoview 1000 confocal microscope. Images were
150 analyzed using ImageJ/Fiji (National Institute of Health, Bethesda, MD) and Photoshop
151 (Adobe, San Jose, CA) software.

152 **(Far) Western Blotting**

153 Cleared cell lysates and EV-enriched fractions were resuspended in PBS, boiled for 5
154 min in Laemmli buffer (10% glycerol, 2% SDS, 10 mM Tris, 10 mM EDTA, bromophenol
155 blue) and fractionated by SDS-PAGE (NuPAGE 4-12% Bis-Tris gels, Invitrogen) before
156 transfer to nitrocellulose membranes (Hybond-C extra, 0.45 µm, GE Healthcare). Cell
157 lysates loaded always corresponded to approximately 20 000 plated cells (day 1) –
158 equivalent to 20 µg protein according to bicinchoninic acid assay (BCA). EV-enriched
159 fractions were collected from 2.4 million plated cells (day 1), unless specified
160 differently. Membranes were probed with primary and HRP-conjugated secondary
161 antibodies or incubated with 11.5 µg/ml recombinant LgBiT (rLgBiT) and 5 µM of
162 Furimazine substrate as described in[14], followed by chemiluminescence detection
163 (Perkin Elmer). Band intensities were quantified using ImageJ by measuring integrated
164 density after background subtraction.

165 **EV uptake (capture/internalization) experiments**

166 ***GFP11-syntenin delivery***

167 CCM sEVs prepared from HEK293 cells transiently overexpressing GFP11-fusions
168 were incubated in serum-free DMEM for 4 hours with recipient MCF-7 GFP1-10 cells
169 at a ratio of 30 producing cells per recipient cells (30p/r) as counted by Countess 3
170 automatic cell counter (ThermoFisher; 16812556) at the time of secretome collection
171 (HEK293 cells) and at the time of sEV addition (MCF-7 cells). Recipient cells were
172 plated on 8-well glass chamber slides the day before and washed with serum-free
173 medium before the start of the experiment. Following the incubation with CCM sEVs
174 or 100K particles, recipient cells were washed with PBS and prepared for confocal
175 microcopy as described above. DAPI or Cell mask deep red signals were used to

176 determine the GFP positivity percentage, all counted values can be found in
177 Supplementary Table 1.

178 ***Full HiBiT dose measurement***

179 To measure the total dose of HiBiT-sEV, an aliquot (1/20) of the CCM sEVs preparation
180 was taken and incubated with 2.5 µg of rLgBiT + 0.05% of Triton X-100 followed by
181 Furimazine substrate for 5 min as determined in [14] before the luminescence
182 measurement.

183 ***HiBiT/NL fusion sEV delivery***

184 CCM sEVs of NL- or HiBiT- fusion overexpressing HEK293 cells were incubated with
185 MCF-7 LgBiT or wild-type recipient cells at 30p/r (see above), for different periods of
186 time, as indicated. Cells were washed three times with versene (Gibco), trypsinized,
187 unless specified differently, pelleted and washed three times with OptiMEM (Fisher
188 sciences) at 500 x g for 5 mins at 4°C, followed by incubation with Furimazine for 5
189 min before the luminescence measurement on a Victor Nivo plate reader
190 (PerkinElmer). For the cytosolic delivery, the cells were split in two halves and these
191 halves were washed three times with OptiMEM. One half was used to measure the EV
192 uptake/internalization by incubating the cells with 2.5 µg of rLgBiT in the presence of
193 2% of Triton X-100 after setup (see Supplementary Figs. 5c, d) and 8.3 µM of
194 Furimazine for 5 min before measurement of luminescence. The other half was used
195 to measure the cytosolic delivery by incubating the cells solely with membrane-
196 permeant Furimazine before measurement of luminescence. For simplified cytosolic
197 delivery assay cells were washed twice before trypsin treatment and once after trypsin
198 treatment. For the measurement of the 'cytosolic delivery' fraction, cells were incubated
199 solely with Furimazine. For the measurement of the 'total sEV uptake' fraction, cells
200 were incubated with 0.8% of Triton X-100 followed by addition of Furimazine substrate.
201 Each CCM sEV preparation served for 1-3 independent measurements of
202 internalization and cytosolic delivery with at least 2 technical repeats.

203 **Statistical analysis**

204 Statistical comparisons were performed using ANOVA followed by Tukey's or Dunnet's
205 multiple comparison test or Student T-test. Graphs depict means or medians with SEM

206 or maximal and minimal values from at least three independent experiments, unless
207 otherwise stated. Statistical analyses were conducted using GraphPad Prism v9.0.

208 **Results**

209 **sEVs fractions from HEK293 cells overexpressing GFP11-syntenin support GFP**
210 **fluorescence reconstitution in MCF-7 cells expressing GFP1-10**

211 To determine whether sEV-embedded syntenin is delivered to the cytosol of recipient
212 cells, we first used a Green Fluorescent Protein (GFP) complementation assay. This
213 assay works on the principle that GFP can be split into two non-fluorescent fragments,
214 a 16 amino-acid peptide (GFP11) and a 214 amino-acid peptide (GFP1-10)[15] (Fig. 1a,
215 left). Cytosolic delivery of sEVs containing GFP11-syntenin into GFP1-10-expressing
216 recipient cells is expected to result in GFP reconstitution, thereby providing a direct
217 spatial readout for cytosolic delivery of syntenin (Fig. 1a, right). We first prepared MCF-
218 7 cells stably expressing GFP1-10 (Supplementary Fig. 1a) and confirmed that upon
219 transfection of expression vectors for GFP11 fusion constructs, we detect GFP
220 fluorescence in these cells (Supplementary Fig. 1b). Transfection of an expression
221 vector encoding GFP11 peptide alone (Supplementary Fig. 1c) did not lead to GFP
222 fluorescence, consistent with the reported instability of this peptide when taken in
223 isolation[16].

224 Having validated the assay, we transfected HEK293 cells (sEV donor cells) with either
225 an empty vector (Mock), an expression vector encoding GFP11-syntenin as the sEV
226 cargo of interest, or an expression vector encoding GFP11-CD63, which has been
227 previously reported to undergo cytosolic delivery and was therefore included as a
228 reference cargo for comparison[17,18]. HEK293 conditioned media were cleared for cell
229 debris and large EVs (lEVs, 10K particles) and either concentrated by low-speed
230 centrifugation on columns or ultracentrifugation. The concentrated conditioned medium
231 is further referred to as CCM sEVs and the ultracentrifuged pellet is further referred to
232 as 100K particles (Fig. 1b). Expression of the different constructs, and their specific
233 sorting in CCM sEVs or 100K particles was analyzed by Western blot (Fig. 1c,
234 Supplementary Fig. 2). While no signal was observed in the 10K pellet, GFP11-
235 syntenin was found to accumulate in CCM sEVs, and in 100K particles.

236 We then incubated HEK293-derived CCM sEVs or 100K particles (derived from the
237 same conditioned medium) with MCF cells expressing GFP1-10, at a dose of 30

238 producing (p) HEK293 cells per recipient (r) MCF7 cell (30p/r) for 4 hours (Fig. 1a) and
239 assessed the reconstitution of GFP fluorescence. As expected, we observed no GFP
240 signal with the Mock (Fig. 1d, e, Supplementary Fig. 3a), and GFP11-CD63 CCM sEVs
241 and 100K particles supported GFP reconstitution (Supplementary Fig. 3b, c). GFP
242 reconstitution was also readily detected upon incubation with GFP11-syntenin CCM
243 sEVs (Fig. 1d, e). Quantification revealed that 9.4 +/- 1.9% of MCF-7 GFP1-10 cells
244 incubated with GFP11-syntenin CCM sEVs displayed GFP fluorescence (Fig. 1d, left),
245 whereas only 3.9 +/- 0.3% of the cells incubated with GFP11-syntenin 100K particles
246 were GFP positive (Fig. 1e, left). Notably, GFP signals induced by GFP11-syntenin
247 CCM sEVs appeared concentrated in dotty intracellular patterns, whereas GFP signals
248 induced by GFP11-syntenin 100K particles had dispersed nuclear localization (Fig. 1d,
249 e).

250 Taken together, these data indicate that sEV syntenin can be delivered to the cytosol
251 of recipient cells, and that ultracentrifugation may alter this delivery.

252 **Nanoluciferase complementation assays measuring CCM sEV HiBiT-syntenin**
253 **dose**

254 To complement these GFP assays with a more quantitative approach, we used
255 Nanoluciferase (NL) based assays[19,20]. Similar to GFP, NL can be split into two non-
256 functional fragments: HiBiT (11 amino acids) and LgBiT (159 amino acids) (Fig. 2a).
257 We prepared expression vectors encoding HiBiT fused to the N-terminus of syntenin
258 or CD63 as a reference cargo. Cell lysates (CL), lEVs (10K), and CCM sEVs from
259 HEK293 cells transiently overexpressing these constructs were analyzed for the
260 presence of HiBiT-tagged proteins by Far-Western blot using recombinant LgBiT
261 (rLgBiT) and Furimazine as substrate (Fig. 2b, Supplementary Fig. 4a). Signals at the
262 expected molecular weights were detected in CL and CCM sEVs but not in lEVs (10K),
263 indicating selective enrichment of HiBiT-tagged syntenin and CD63 in sEV fractions.

264 Next, we established experimental conditions allowing to quantify the amount of HiBiT
265 in sEVs by luminescence. We observed that, in the presence of 1.66 μM Furimazine
266 (membrane permeant substrate for NL), 0.05% Triton X-100 detergent, and 2.5 μg
267 rLgBiT (recombinant form used to saturate HiBiT), luminescence signals were directly
268 proportional with the reagent dilution (Supplementary Fig. 4b, c). To determine optimal
269 reagent concentrations (Fig. 2c), we tested different dilutions of CCM sEVs and

270 decided to use a 1/20 dilution (within the linear range), to measure the total sEV dose
271 in subsequent experiments.

272 CCM sEVs were then incubated in the presence (0.05%) or absence of Triton X-100
273 (Fig. 2d). Luminescence was detected only when both detergent and rLgBiT were
274 added (Fig. 2e). These results indicate the HiBiT-syntenin is completely embedded
275 within sEVs. Similar observations were obtained for HiBiT-CD63, consistent with the
276 cytosolic orientation of its N-terminus. Full-length NL fused to syntenin served as a
277 positive control.

278 Together, these data establish that HiBiT-syntenin is strictly embedded within CCM
279 sEVs and can be robustly quantified by luminescence following sEV permeabilization
280 and NL complementation.

281 **Establishing conditions for measuring internalized sEVs**

282 To distinguish between 'captured' (retained, but non-internalized) and internalized
283 sEVs, we treated the recipient cells with trypsin. As we and others documented that
284 heparan sulfate proteoglycans (HSPGs) are major receptors for sEV uptake[6,21], and
285 as HSPGs are highly trypsin sensitive, we expected that trypsin treatment would
286 remove cell-surface captured sEVs. Recipient MCF-7 cells were therefore first
287 incubated with NL-syntenin CCM sEVs, washed to remove unbound vesicles, and then
288 treated with trypsin and washed again. When NL-syntenin CCM sEVs (30p/r) were
289 incubated with MCF-7 wild-type (WT) cells, luminescence signals measured after the
290 washing of the cells in the absence of trypsinization continued to increase over time,
291 without reaching equilibrium. In contrast, when cells were treated with trypsin and
292 washed, luminescence signals were reaching a plateau after 60 minutes and remained
293 stable for up to 4 hours (Fig. 3a).

294 These results indicate that a substantial fraction of the signal measured without
295 trypsinization originates from 'captured' sEVs, bound to or trapped between cells.

296 Next, to address cytosolic delivery, we generated MCF-7 cells stably expressing
297 cytosolic LgBiT (Supplementary Fig. 5a). We first tested whether NL complementation
298 could be detected upon transfection with expression vectors encoding HiBiT-syntenin
299 or HiBiT-CD63. Empty vector (Mock) was used as a negative control and NL-syntenin
300 was used as a technical control (Supplementary Fig. 5b). Although Mock-transfected

cells displayed high background luminescence, signals were more than two orders of magnitude higher in cells transfected with expression vectors encoding HiBiT-syntenin or HiBiT-CD63, confirming that NL complementation can occur and can be measured.

We next set up experimental conditions to measure the total internalized (not necessarily release in the cytosol) syntenin sEV fraction. We found that Triton X-100 concentrations between 0.5–2%, in the presence of 2.5 µg rLgBiT, provided stable and reproducible luminescence signals (Supplementary Fig. 5c, d).

Taken together, these set-up experiments indicate that it is possible to measure reconstituted NL luminescence in MCF-7 LgBiT cells, including in the presence of detergent.

**Internalization and cytosolic delivery of sEV HiBiT-syntenin in MCF-7 cells expressing LgBiT**

Having defined conditions to measure the internalized syntenin sEV fractions, we incubated recipient MCF-7 LgBiT cells with HiBiT- syntenin CCM sEVs for 4 hours (30p/r) and compared three distinct experimental parameters: (i) the total administered HiBiT sEV dose, (ii) the internalized fraction (measured after trypsinization and detergent permeabilization), and (iii) the cytosolic fraction (measured after trypsinization in the absence of detergent) (Fig. 3b).

Luminescence signals are shown in Fig. 3c (raw data in Supplementary Table 2). For HiBiT-syntenin, quantitative analysis revealed that only ~0.03% of the administered CCM sEV dose was internalized by MCF-7 LgBiT cells within 4 hours, whereas cytosolic delivery represented 84.7 +/- 36.3% of the internalized sEV fraction. Although variability between experiments was observed, cytosolic delivery consistently represented a large fraction of the internalized pool across biological replicates. For NL-syntenin CCM sEVs (technical control), signal corresponding to ~0.01% of the total dose was detected following detergent permeabilization of MCF-7 LgBiT cells, while 70.8 +/- 8.5% of the internalization signal was detected in the absence of detergent (Fig. 3c). For HiBiT-CD63 (used as positive control), the internalization was ~0.02% compared to the full dose and cytosolic delivery was 31.9 +/- 12.4% of the internalized fraction (Supplementary Fig. 5e).

Taken together, these results show that solely a small fraction of the administered sEV dose is internalized, while a large fraction of the internalized pool undergoes cytosolic delivery.

**Syntenin molecular determinants supporting cytosolic delivery**

We then investigated molecular determinants within syntenin that support cytosolic delivery. Fortunately, mutants were found in equivalent amounts in CCM sEVs, as sEV HiBiT-syntenin total dose measurements were similar for WT and mutant constructs (Supplementary Fig. 6b, raw data in Supplementary Table 2).

First, we examined whether binding of syntenin to the fusogenic lipid phosphatidic acid (PA), via its PDZ1[8], contributes to cytosolic delivery. A syntenin mutant containing two lysine-to-alanine substitutions within the putative PA-binding site of PDZ1 was generated (Fig. 4a, Supplementary Fig. 6a). These mutations did not significantly alter cytosolic delivery efficiency in recipient cells compared to WT syntenin (Fig. 4b). We next investigated the role of the N-terminal domain, as this domain interacts with Alix, and a report has implicated Alix in back-fusion of intraluminal vesicles with the limiting endosomal membrane[22]. We first prepared a syntenin mutant with deletion of this domain (ΔNterm). Cytosolic delivery of this mutant was below the background signals obtained with Mock CCM sEVs, suggesting that deletion of the N-terminal domain completely abolishes cytosolic delivery.

Next, we tested an Alix-binding-deficient syntenin mutant in which the three N-terminal LYP motifs were replaced by LAA[5]. Unexpectedly, this mutation did not affect cytosolic delivery efficiency compared to WT syntenin (Fig. 4b). Finally, because the N-terminal domain also contains the Src phosphorylation site tyrosine-46[11], we also tested the cytosolic delivery of Src phosphorylation-deficient (Y46F) or phosphorylation-mimetic (Y46E) syntenin mutants. Surprisingly, cytosolic delivery of the Y46F mutant was significantly increased compared to WT syntenin, whereas cytosolic delivery of the Y46E mutant was completely abolished (Fig. 4b).

Taken together, these results indicate that the N-terminal domain of syntenin is essential for cytosolic delivery and that the phosphorylation status of tyrosine-46 functions as a molecular switch, with phosphorylation inhibiting and dephosphorylation promoting cytosolic delivery.

362 **Discussion**

363 In this study, we demonstrate that sEV-embedded syntenin undergoes delivery to the
364 cytosol of recipient cells. Using a GFP complementation assay, we observed cytosolic
365 delivery of sEV-embedded syntenin in ~9% of recipient cells within 4 hours (Fig. 1d)
366 upon incubation with relatively low amounts of GFP11-syntenin CCM sEVs (secretome
367 of 30 producing cells per recipient cell (30p/r). This relatively high fraction of GFP-
368 positive cells is striking given the generally low efficiencies reported for sEV-mediated
369 cargo transfer. While one could argue that high efficiency of GFP reconstitution might
370 result from transfer of DNA encoding GFP11-syntenin[23], the short incubation time,
371 together with the requirement for cytosolic protein complementation, makes de novo
372 transcription, translation, and subsequent GFP reconstitution highly unlikely. In other
373 words, we are confident that GFP reconstitution can be solely explained by the transfer
374 of GFP11-syntenin protein from donor cells to the cytosol of recipient cells expressing
375 GFP1-10.

376 Our GFP reconstitution assays also highlight that the method of sEV preparation may
377 influence syntenin delivery. Noteworthy, we observed that recipient cells treated with
378 GFP11-syntenin CCM sEVs displayed nuclear and cytosolic dotty GFP patterns. These
379 cytosolic dots may be explained by efficient local GFP reconstitution driven by
380 membrane-associated clustering of GFP11-syntenin, consistent with the known
381 enrichment of syntenin in microsomal fractions[2] and its interaction with various
382 lipids[8,24,25]. Accordingly, GFP reconstitution mediated by cytosolic GFP11-syntenin
383 molecules that are not membrane-associated may remain below the detection
384 threshold of this microscopy assay. Interestingly, both dotty and nuclear distributions
385 are reminiscent of endogenous syntenin distribution[2].

386 To complement this spatially resolved but poorly quantitative approach with a more
387 sensitive and flexible approach, we used Nanoluciferase (NL) and a NL-
388 complementation assay[26]. Using this assay, we first established that HiBiT-syntenin is
389 strictly embedded within sEVs (Fig. 2d), thereby excluding non-vesicular delivery of
390 syntenin. Using NL-syntenin sEVs we show that capture exceeds internalization by
391 nearly one order of magnitude within the first hours (Fig. 3a), and fails to reach
392 equilibrium over time. Heparan sulfate proteoglycans are thought to play a prominent
393 role in the capture and internalization of sEVs[7,21]. Because recipient cells were freshly
394 plated prior to sEV addition, it is plausible that heparan sulfate proteoglycan

395 abundance or accessibility at the cell surface increases over time, which may
396 contribute to the progressive increase of the captured signal. As heparan sulfate
397 proteoglycans are highly protease-sensitive[27], trypsin digestion is expected to remove
398 (most of) the capture-associated signal. The remaining signal (here considered as
399 internalized fraction), in contrast to capture, rapidly reaches a plateau value and
400 remains stable over time (Fig. 3a). Internalization reaching rapid equilibrium implies
401 that the internalized (NL) cargo is metabolically unstable (i.e. is degraded and/or is
402 again leaving cells). Thus, (at least here) capture dominates early sEV-cell interactions
403 and can mask the comparatively limited internalization process. This separation
404 between capture and internalization is critical for interpreting sEV delivery
405 measurements. Notably, while we previously showed that total 'uptake' (capture plus
406 internalization combined) can be saturated when high sEV doses are applied[14],
407 whether increasing sEV dose also enhances internalization remains an open question.

408 After clarifying the importance of separating sEV capture from internalization, we
409 incubated CCM sEVs with recipient MCF-7 LgBiT cells and found that (at equilibrium)
410 the internalized HiBiT-syntenin corresponds to only a very small fraction (~0.03%) of
411 the administered HiBiT-syntenin sEV dose. Yet relative to this internalized fraction,
412 cytosolic delivery of this syntenin was extremely effective (85%) (Fig. 3c).

413 These observations were unexpected in light of the studies stating that cytosolic
414 delivery is negligible in the absence of viral fusogenic proteins, whereas the
415 internalization is efficient[20,28–30]. Of note, these conclusions are often based on
416 microscopy-based readouts that do not measure the total administered dose[30], lack
417 correction for background luminescence[29], or do not distinguish between capture and
418 internalization[31].

419 In contrast, our findings are consistent with those of Bonsergent et al., who similarly
420 concluded that internalization, rather than cytosolic delivery, represents the limiting
421 step of sEV cargo delivery[32]. That study did not use split reconstitution assays but used
422 cell fractionation and an HSP70 NL fusion protein. Of note, syntenin was shown to
423 govern HSP70 loading into sEVs[5]. As such HSP70 and syntenin sEVs may be very
424 similar[33], and the efficient cytosolic delivery observed for HSP70 may therefore reflect
425 intrinsic properties of the syntenin-dependent sEV subtype, which can represent up to
426 50% of sEVs[5,11]. Together, these data clearly indicate that cytosolic delivery does not
427 necessarily require viral fusogenic proteins.

428 We also started to address the molecular mechanisms supporting sEV syntenin
429 cytosolic delivery in sEV recipient cells. Given the established role of phosphatidic acid
430 (PA) binding in syntenin-dependent sEV biogenesis via the PDZ1 domain, and the
431 suggested role of phosphatidic acid in membrane fusion events[34–36], we investigated
432 whether syntenin-PA interaction may contribute to cytosolic delivery but found no
433 evidence supporting this hypothesis (Fig. 4b). In contrast, deletion of the N-terminal
434 domain abolished syntenin cytosolic delivery, suggesting that this domain is required
435 either to generate cytosolic delivery-competent sEVs or to support cytosolic delivery
436 following internalization. Of note, syntenin lacking its N-terminal domain was also
437 shown to promote sEV biogenesis[37], but based on our data, these sEVs would most
438 probably be cytosolic delivery-incompetent. The N-terminal domain is responsible for
439 Alix binding, which has been proposed to be involved in intraluminal back-fusion and
440 thereby may convey cytosolic delivery[22]. Nevertheless, when syntenin is mutated at its
441 Alix binding sites, it still efficiently undergoes cytosolic delivery. Knock-out of
442 endogenous syntenin may be required to completely exclude a role for Alix as both
443 mutant and endogenous syntenin may belong to the same membrane domains.
444 Interestingly, the N-terminal domain also contains tyrosine-46, which we previously
445 identified as a Src phosphorylation site[11]. A phosphorylation-mimetic mutation (Y46E)
446 abolishes cytosolic delivery, whereas a phosphorylation-deficient mutation (Y46F)
447 promotes cytosolic delivery. These data indicate that tyrosine-46 functions as a
448 molecular switch for cytosolic delivery and suggest that Src may dampen the
449 'fusogenic' properties of sEVs toward recipient cells. Considering that Src promotes
450 pro-migratory activities of sEVs[11], a corollary of these observations is that the pro-
451 migratory activity of sEVs may be unrelated to their 'fusogenic' activity, and thus to the
452 release of specific molecules present inside sEVs. By extension, the pro-migratory
453 activity of sEVs may instead rely on contact-dependent signaling and/or metabolic
454 effects after lysosomal degradation. These exciting considerations require further
455 investigations.

456 We also assessed cytosolic delivery of CD63. Although CD63 and syntenin directly
457 interact[38] and may thus be present on the same sEV subtype, CD63, compared to
458 syntenin, showed lower cytosolic delivery as measured by NL complementation
459 (Supplementary Fig. 5e). This might be due to HiBiT tag cleavage (Fig. 2b), which can
460 render complementation inefficient even when these sEVs reach the cytosol. Such

461 cleavage, together with indirect cytosolic delivery measurements (e.g. using Cre
462 activity as a cytosolic delivery readout) or overestimation of internalization, may explain
463 the inconsistent CD63 cytosolic delivery efficiencies[17,18,28,30,39]. Alternatively, for
464 reasons that remain unclear, CD63 release from sEVs may be inefficient, consistent
465 with the need for CD63-cleavable constructs reported by others[30,40,41].

466 Independently of these conceptual considerations, our study also establishes a
467 quantitative assay to measure sEV-mediated internal cargo delivery. However, our
468 experience demonstrates that several technical aspects can be laborious and should
469 be carefully considered before implementation. In particular, as detergent is required
470 to quantify both the total dose and internalized fraction of sEV HiBiT-syntenin,
471 experiments should be carefully set-up. Indeed, when Triton X-100 is used,
472 luminescence increased at low detergent concentrations before returning to baseline
473 at higher levels (Supplementary Fig. 3d), highlighting the need to define appropriate
474 detergent ranges. Endogenous LgBiT levels in recipient cells were insufficient to
475 support NL reconstitution under these conditions (Supplementary Fig. 3e),
476 necessitating recombinant LgBiT supplementation. Luminescence derived from
477 reagents also creates background signal, underscoring the need for stringent controls.
478 Together, these considerations emphasize that although NL complementation provides
479 high sensitivity, careful optimization is essential for its reliable application to sEV
480 delivery studies.

481 In conclusion, we identify a novel function of syntenin as a mediator of sEV cytosolic
482 delivery and establish a quantitative assay for assessing this delivery. Together, our
483 findings illustrate that the method of sEV preparation affects sEV internal cargo delivery
484 and, by extension, likely sEV function. They indicate that sEV-syntenin capture is slow
485 in reaching equilibrium and (although specific) may thus be more complex than simple
486 cell surface-binding; that internalization is rapid in reaching equilibrium, but minimal
487 when considering the administered dose; and that syntenin supports efficient cytosolic
488 delivery through a tyrosine located in its N-terminal domain, which functions as a
489 switch. Clearly, syntenin supports cytosolic delivery without requiring fusion to viral
490 proteins, highlighting its potential as a biologically relevant scaffold for sEV-mediated
491 cytosolic cargo delivery. Our study also supports the notion that enhancing sEV
492 internalization may help increasing the overall sEV delivery. That issue may thus be
493 the first priority from an EV-therapeutic based perspective.

494 **Data availability statement**

495 The data generated in this study are available from the corresponding author upon
496 request.

497 **Acknowledgements**

498 The authors thank Antonio-Egea Jimenez for mapping of the syntenin putative PA-
499 binding domain. We also thank Clotilde Thery for useful discussions regarding our
500 work. This research project was funded by Kom op tegen Kanker (Stand up to Cancer),
501 the Flemish cancer society (projectID: 12367) and the internal funds of the KU Leuven
502 (C14/20/105). L.H. is a PhD Fellow of the Research Foundation – Flanders (FWO,
503 1SE2422N). Schemes were created using BioRender.com.

504 **Author contribution**

505 P.Z., G.D. and L.H. conceived and designed the study and wrote the manuscript; L.H.,
506 E.J and S.M. performed experiments and analyzed the data. G.D., C.T, A.J, P.Z., and
507 L.H. provided critical suggestions and revised the manuscript. All authors read and
508 approved the final manuscript.

509 **Additional information**

510 Competing Interests Statement

511 P.Z., G.D. and L.H. are inventors of the patent PCT/EP2023/050644 related to this
512 work. E.J, S.M., C.T., and A. J. declare no competing conflicts of interests.

513 **Reference**

514 1. Ngo, J. M. *et al.* Extracellular Vesicles and Cellular Homeostasis. *Annu. Rev.*
515 *Biochem.* **94**, 587–609 (2025).
516 2. Zimmermann, P. *et al.* Characterization of Syntenin, a Syndecan-binding PDZ
517 Protein, as a Component of Cell Adhesion Sites and Microfilaments. *Mol. Biol.*
518 *Cell* **12**, 339–350 (2001).
519 3. Geijsen, N. *et al.* Cytokine-specific transcriptional regulation through an IL-
520 5Ralpha interacting protein. *Science* **293**, 1136–1138 (2001).

521 4. Kashyap, R. *et al.* Syntenin controls migration, growth, proliferation, and cell cycle
522 progression in cancer cells. *Front. Pharmacol.* **6**, (2015).
523 5. Baietti, M. F. *et al.* Syndecan-syntenin-ALIX regulates the biogenesis of
524 exosomes. *Nat. Cell Biol.* **14**, 677–685 (2012).
525 6. Castro-Cruz, M. *et al.* PDZ scaffolds regulate extracellular vesicle production,
526 composition, and uptake. *Proc. Natl. Acad. Sci. U. S. A.* **120**, e2310914120
527 (2023).
528 7. Kashyap, R. *et al.* Syntenin-knock out reduces exosome turnover and viral
529 transduction. *Sci. Rep.* **11**, 4083 (2021).
530 8. Ghossoub, R. *et al.* Syntenin-ALIX exosome biogenesis and budding into
531 multivesicular bodies are controlled by ARF6 and PLD2. *Nat. Commun.* **5**, 3477
532 (2014).
533 9. Grootjans, J. J. *et al.* Syntenin, a PDZ protein that binds syndecan cytoplasmic
534 domains. *Proc. Natl. Acad. Sci.* **94**, 13683–13688 (1997).
535 10. Bishop, J. R., Schuksz, M. & Esko, J. D. Heparan sulphate proteoglycans fine-
536 tune mammalian physiology. *Nature* **446**, 1030–1037 (2007).
537 11. Imjeti, N. S. *et al.* Syntenin mediates SRC function in exosomal cell-to-cell
538 communication. *Proc. Natl. Acad. Sci.* **114**, 12495–12500 (2017).
539 12. Kugeratski, F. G. *et al.* Quantitative proteomics identifies the core proteome of
540 exosomes with syntenin-1 as the highest abundant protein and a putative
541 universal biomarker. *Nat. Cell Biol.* **23**, 631–641 (2021).
542 13. Charrin, S. *et al.* The Major CD9 and CD81 Molecular Partner: IDENTIFICATION
543 AND CHARACTERIZATION OF THE COMPLEXES. *J. Biol. Chem.* **276**, 14329–
544 14337 (2001).

14. Hyka, L. *et al.* A syndecan-based genetic approach to coat the surface of small extracellular vesicles with Nanobodies. 2026.01.29.702589 Preprint at https://doi.org/10.64898/2026.01.29.702589 (2026).
15. Ghosh, I., Hamilton, A. D. & Regan, L. Antiparallel Leucine Zipper-Directed Protein Reassembly: Application to the Green Fluorescent Protein. *J. Am. Chem. Soc.* **122**, 5658–5659 (2000).
16. Lévrier, A. *et al.* Split Reporters Facilitate Monitoring of Gene Expression and Peptide Production in Linear Cell-Free Transcription–Translation Systems. *ACS Synth. Biol.* **13**, 3119–3127 (2024).
17. Joshi, B. S., de Beer, M. A., Giepmans, B. N. G. & Zuhorn, I. S. Endocytosis of Extracellular Vesicles and Release of Their Cargo from Endosomes. *ACS Nano* **14**, 4444–4455 (2020).
18. Perrin, P. *et al.* Retrofusion of intralumenal MVB membranes parallels viral infection and coexists with exosome release. *Curr. Biol. CB* **31**, 3884-3893.e4 (2021).
19. Dixon, A. S. *et al.* NanoLuc Complementation Reporter Optimized for Accurate Measurement of Protein Interactions in Cells. *ACS Chem. Biol.* **11**, 400–408 (2016).
20. Somiya, M. & Kuroda, S. Real-Time Luminescence Assay for Cytoplasmic Cargo Delivery of Extracellular Vesicles. *Anal. Chem.* **93**, 5612–5620 (2021).
21. Christianson, H. C., Svensson, K. J., van Kuppevelt, T. H., Li, J.-P. & Belting, M. Cancer cell exosomes depend on cell-surface heparan sulfate proteoglycans for their internalization and functional activity. *Proc. Natl. Acad. Sci. U. S. A.* **110**, 17380–17385 (2013).

569 22. Bissig, C. & Gruenberg, J. ALIX and the multivesicular endosome: ALIX in
570 Wonderland. *Trends Cell Biol.* **24**, 19–25 (2014).
571 23. Bergsmedh, A. *et al.* Horizontal transfer of oncogenes by uptake of apoptotic
572 bodies. *Proc. Natl. Acad. Sci.* **98**, 6407–6411 (2001).
573 24. Egea-Jimenez, A. L. *et al.* Frizzled 7 and PIP2 binding by syntenin PDZ2 domain
574 supports Frizzled 7 trafficking and signalling. *Nat. Commun.* **7**, 12101 (2016).
575 25. Zimmermann, P. *et al.* PIP(2)-PDZ domain binding controls the association of
576 syntenin with the plasma membrane. *Mol. Cell* **9**, 1215–1225 (2002).
577 26. Teo, S. L. Y. *et al.* Unravelling cytosolic delivery of cell penetrating peptides with a
578 quantitative endosomal escape assay. *Nat. Commun.* **12**, 3721 (2021).
579 27. Brucato, S. *et al.* Biochemical characterization of integral membrane heparan
580 sulfate proteoglycans in Sertoli cells from immature rat testis. *Biochim. Biophys.*
581 *Acta BBA - Biomembr.* **1510**, 474–487 (2001).
582 28. de Jong, O. G. *et al.* A CRISPR-Cas9-based reporter system for single-cell
583 detection of extracellular vesicle-mediated functional transfer of RNA. *Nat.*
584 *Commun.* **11**, 1113 (2020).
585 29. Hirose, H., Hirai, Y., Sasaki, M., Sawa, H. & Futaki, S. Quantitative Analysis of
586 Extracellular Vesicle Uptake and Fusion with Recipient Cells. *Bioconjug. Chem.*
587 **33**, 1852–1859 (2022).
588 30. Liang, X. *et al.* Engineering of extracellular vesicles for efficient intracellular
589 delivery of multimodal therapeutics including genome editors. *Nat. Commun.* **16**,
590 4028 (2025).
591 31. Inano, S. & Kitano, T. A modified CD9 tag for efficient protein delivery via
592 extracellular vesicles. *PLOS ONE* **19**, e0310083 (2024).

32. Bonsergent, E. *et al.* Quantitative characterization of extracellular vesicle uptake and content delivery within mammalian cells. *Nat. Commun.* **12**, 1864 (2021).
33. Kim, O., Hwangbo, C., Tran, P. T. & Lee, J.-H. Syntenin-1-mediated small extracellular vesicles promotes cell growth, migration, and angiogenesis by increasing onco-miRNAs secretion in lung cancer cells. *Cell Death Dis.* **13**, 122 (2022).
34. Kooijman, E. E., Chupin, V., de Kruijff, B. & Burger, K. N. J. Modulation of membrane curvature by phosphatidic acid and lysophosphatidic acid. *Traffic* **4**, 162–174 (2003).
35. Zeniou-Meyer, M. *et al.* Phospholipase D1 Production of Phosphatidic Acid at the Plasma Membrane Promotes Exocytosis of Large Dense-core Granules at a Late Stage*. *J. Biol. Chem.* **282**, 21746–21757 (2007).
36. Egea-Jimenez, A. L. & Zimmermann, P. Phospholipase D and phosphatidic acid in the biogenesis and cargo loading of extracellular vesicles. *J. Lipid Res.* **59**, 1554–1560 (2018).
37. Ai, Y. *et al.* Endocytosis blocks the vesicular secretion of exosome marker proteins. *Sci. Adv.* **10**, eadi9156 (2024).
38. Latysheva, N. *et al.* Syntenin-1 Is a New Component of Tetraspanin-Enriched Microdomains: Mechanisms and Consequences of the Interaction of Syntenin-1 with CD63. *Mol. Cell. Biol.* **26**, 7707–7718 (2006).
39. Askarian-Amiri, S., Weissenhorn, W., Sadoul, R. & Chatellard, C. Lack of evidence for cargo release of CD63-EVs into recipient cells. 2025.04.01.646561 Preprint at https://doi.org/10.1101/2025.04.01.646561 (2025).

40. Elsharkasy, O. M. *et al.* A modular strategy for extracellular vesicle-mediated CRISPR-Cas9 delivery through aptamer-based loading and UV-activated cargo release. *Nat. Commun.* **16**, 10309 (2025).

41. Obuchi, W. *et al.* Engineering of CD63 Enables Selective Extracellular Vesicle Cargo Loading and Enhanced Payload Delivery. *J. Extracell. Vesicles* **14**, e70094 (2025).

624 **Main figures**

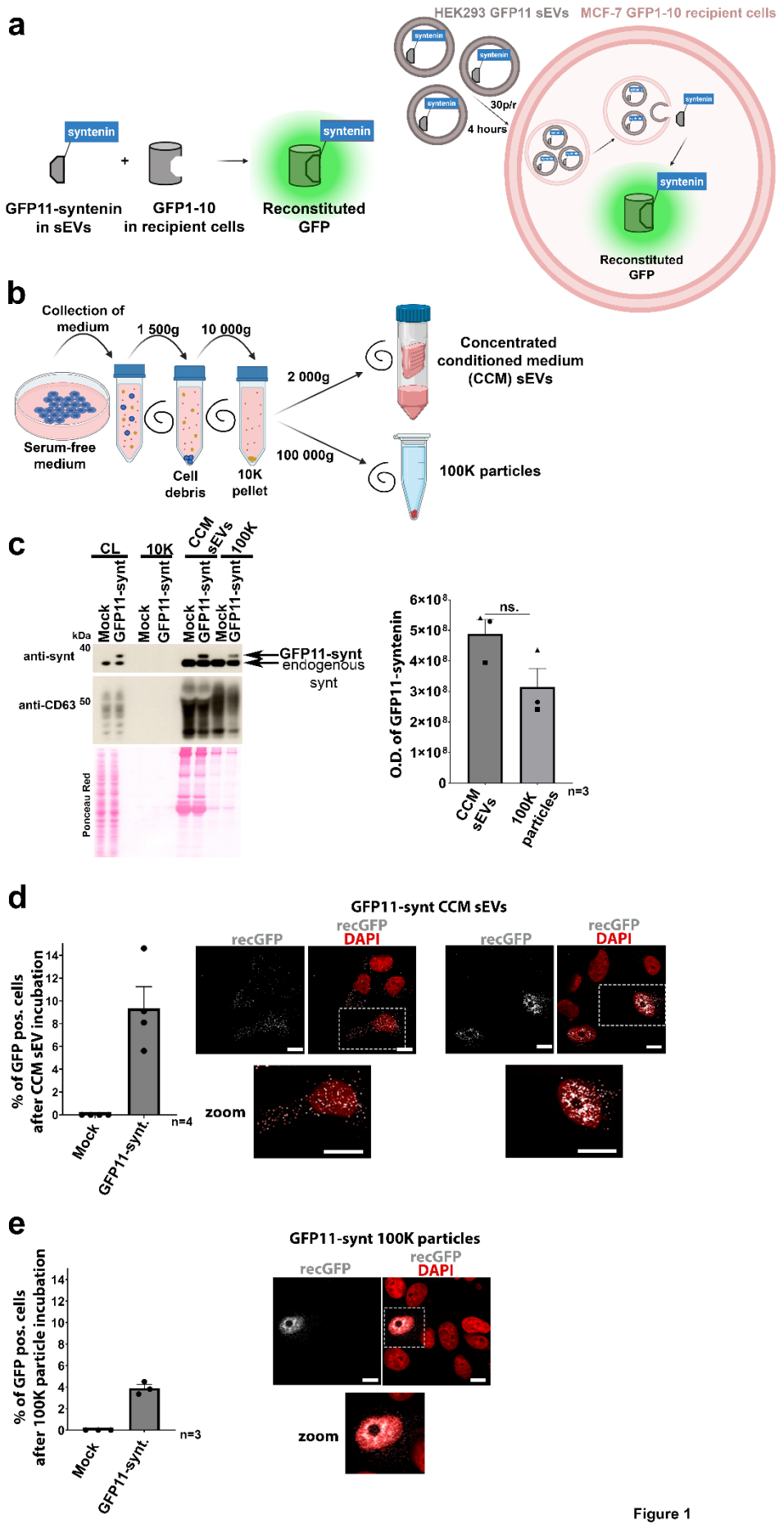
a
HEK293 GFP11 sEVs
MCF-7 GFP1-10 recipient cells
syntenin
GFP11-syntenin in sEVs
GFP1-10 in recipient cells
Reconstituted GFP
30p/r
4 hours
b
Collection of medium
1 500g
10 000g
2 000g
100 000g
Serum-free medium
Cell debris
10K pellet
Concentrated conditioned medium (CCM) sEVs
100K particles
c
CL
10K
CCM sEVs
100K
Mock
GFP11-synt
kDa
anti-synt
anti-CD63
Ponceau Red
GFP11-synt
endogenous synt
O.D. of GFP11-syntenin
ns.
CCM sEVs
100K particles
n=3
d
GFP11-synt CCM sEVs
recGFP
DAPI
zoom
% of GFP pos. cells after CCM sEV incubation
Mock
GFP11-synt.
n=4
e
GFP11-synt 100K particles
% of GFP pos. cells after 100K particle incubation
n=3

Figure 1

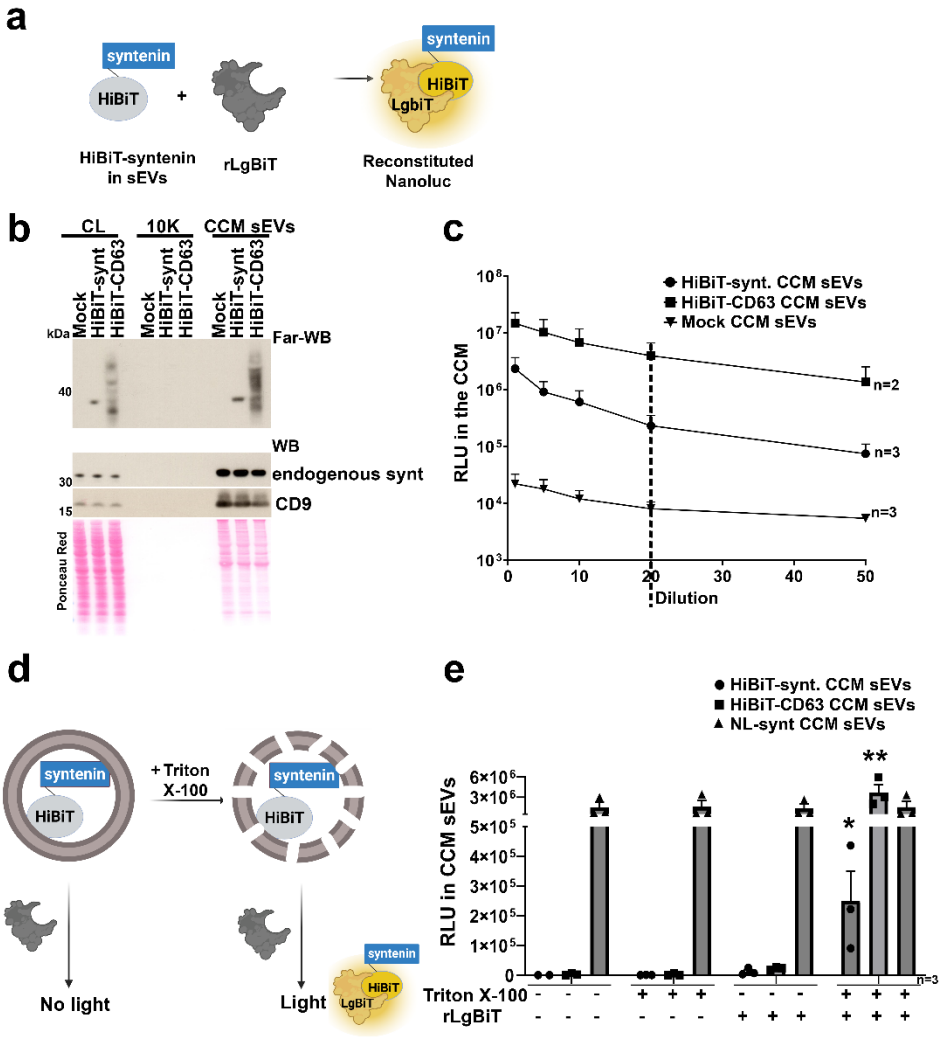
a
syntenin
HiBiT
+
HiBiT-syntenin in sEVs
rLgBiT
syntenin
HiBiT
LgbiT
Reconstituted Nanoluc
b
CL
10K
CCM sEVs
Mock
HiBiT-synt
HiBiT-CD63
kDa
Far-WB
40
WB
30
endogenous synt
15
CD9
Ponceau Red
c
HiBiT-synt. CCM sEVs
HiBiT-CD63 CCM sEVs
Mock CCM sEVs
RLU in the CCM
n=2
n=3
n=3
Dilution
d
syntenin
HiBiT
+Triton X-100
No light
Light
LgBiT
e
HiBiT-synt. CCM sEVs
HiBiT-CD63 CCM sEVs
NL-synt CCM sEVs
RLU in CCM sEVs
Triton X-100
rLgBiT
n=3

Figure 2

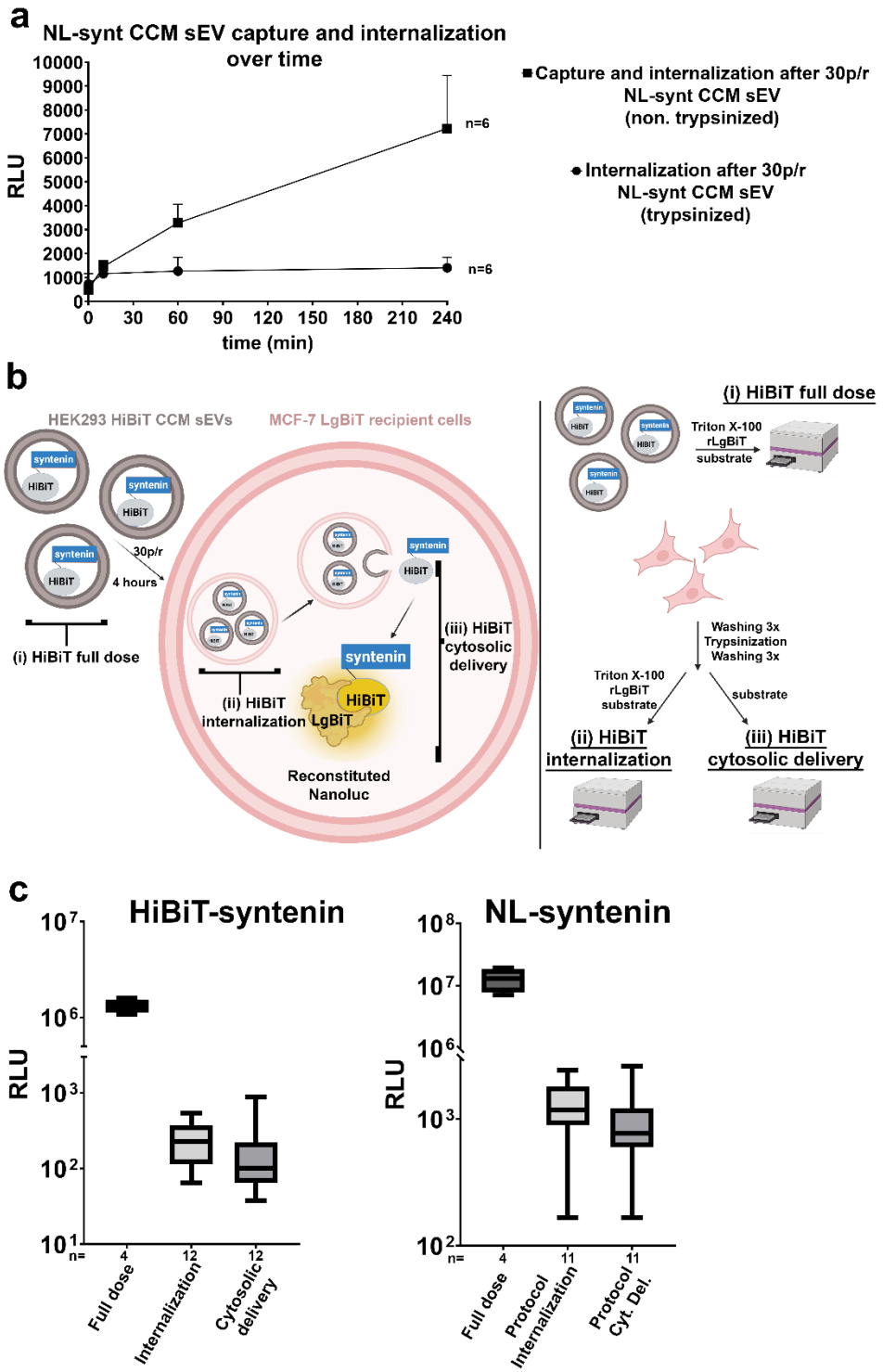
a
NL-synt CCM sEV capture and internalization over time
RLU
time (min)
n=6
n=6
Capture and internalization after 30p/r NL-synt CCM sEV (non. trypsinized)
Internalization after 30p/r NL-synt CCM sEV (trypsinized)
b
HEK293 HiBiT CCM sEVs
MCF-7 LgBiT recipient cells
syntenin
HiBiT
30p/r
4 hours
(i) HiBiT full dose
(ii) HiBiT internalization
(iii) HiBiT cytosolic delivery
LgBiT
Reconstituted Nanoluc
Triton X-100
rLgBiT substrate
Washing 3x
Trypsinization
Washing 3x
substrate
c
HiBiT-syntenin
NL-syntenin
RLU
n=
Full dose
Internalization
Cytosolic delivery
Protocol Internalization
Protocol Cyt. Del.

Figure 3

627

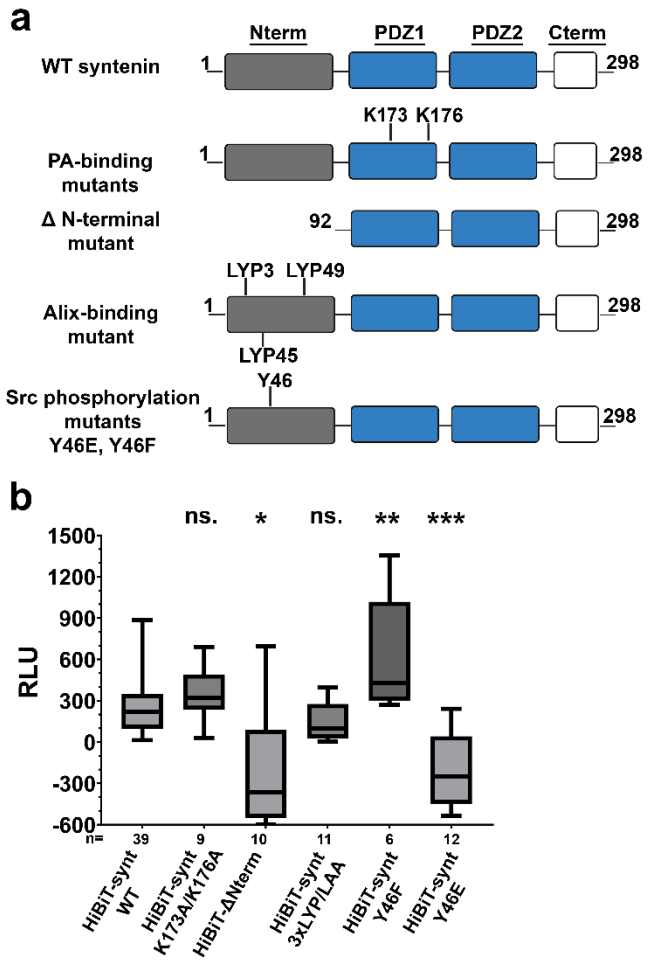
a
Nterm
PDZ1
PDZ2
Cterm
WT syntenin
1
298
K173 K176
PA-binding mutants
Δ N-terminal mutant
92
LYP3 LYP49
Alix-binding mutant
LYP45
Y46
Src phosphorylation mutants Y46E, Y46F
b
ns.
*
ns.
**
***
RLU
1500
1200
900
600
300
0
-300
-600
n=
39
9
10
11
6
12
HiBiT-synt WT
HiBiT-synt K173A/K176A
HiBiT-ΔNterm
HiBiT-synt 3xLYP/LAA
HiBiT-synt Y46F
HiBiT-synt Y46E

Figure 4

630 **Figure legends**

631 **Figure 1. GFP11-syntenin is sorted to small extracellular vesicles (sEVs) and**
632 **supports reconstitution of GFP in recipient cells expressing GFP1-10. (a)**
633 Schematic representation of the GFP complementation assay. GFP can be split into
634 two non-fluorescent fragments (GFP11 and GFP1-10). In our setting, GFP1-10 is
635 stably expressed in the cytosol of recipient MCF-7 cells, GFP11 is fused to syntenin
636 and present in the sEVs of donor HEK293 cells. Fluorescence is reconstituted when
637 the two fragments come in direct contact. MCF-7 cells stably expressing GFP1-10 were
638 incubated with HEK293-derived sEVs at a producing:recipient cell ratio of 30:1 (30p/r).
639 Cells were incubated for 4 hours with the 100K pellet or CCM sEVs of HEK293 cells
640 transiently overexpressing GFP11-syntenin or Mock as control. **(b)** HEK293 sEVs
641 fractions were prepared by differential ultracentrifugation or by concentrating the
642 conditioned media (CCM sEVs) and analyzed by Western blot using anti-syntenin
643 antibodies **(c, left)**. Note that the syntenin signals (endogenous or GFP11-fusion) are
644 present in the 100K and CCM sEVs fractions but absent from 10K pellets. Cell lysates
645 (CL) correspond to 20,000 cells, secretome fractions were prepared from 2.4 million
646 cells. Endogenous syntenin and CD63 were used as markers and loading controls. **(c,**
647 **right)** Bar graph showing average band intensities + SEM of GFP11-syntenin (Y-axis,
648 integrated density) prepared by concentration (CCM sEVs) or by differential
649 ultracentrifugation (100K particles), as indicated. Individual points correspond to
650 individual western blot assays shown in Supplementary Fig. 3. **(d, e)** Left, bar graphs
651 showing the average percentages + SEM of GFP positive MCF-7 GFP1-10 cells after
652 the incubation with Mock or GFP11-syntenin CCM sEVs (d) or 100K particles (e).
653 Individual data points correspond to independent biological repeats and represent
654 values obtained from at least 40 nuclei scored at random. Right, confocal micrographs
655 showing the localization of the GFP fluorescence (grey) in MCF-7 GFP1-10 cells
656 treated with GFP11-syntenin CCM sEVs (d) or 100K particles (e). Nuclei were stained
657 with DAPI (red). Inserts correspond to higher magnifications of indicated areas. Note
658 dotty patterns in the cytosol (left) and the nuclei (right) of the reconstituted GFP
659 followed by CCM sEV incubation **(d)** and nuclear reconstituted GFP patterns followed
660 by 100K particle incubation **(e)**. Scale bar is 10 μm. Related to **Supplementary Figs.**
661 **1, 2 and 3**.

**Figure 2. All HiBiT-syntenin present in the secretome of HEK293 cells is encapsulated within small extracellular vesicles . (a)** Schematic representation of the Nanoluciferase (NL) reconstitution. NL can be split into two non-functional fragments (HiBiT and LgBiT) that reconstitute enzymatic activity upon direct interaction. In this figure, HiBiT is fused to syntenin (CD63, not shown). HEK293 cells are transfected with expression vectors for these constructs and their conditioned media are processed to prepare HiBiT-containing CCM sEVs. **(b)** Top part, Far Western blot analysis of cell lysates (CL) and secretome fractions (10K pellet, CCM sEVs) from HEK293 cells transiently expressing HiBiT-syntenin, HiBiT-CD63, or empty vector (Mock). Blots were probed with recombinant LgBiT (rLgBiT) before Furimazine substrate was added, to reconstitute NL and generate luminescence signals. CL corresponds to 20,000 cells, secretome fractions were prepared from 3.6 million cells. Bottom part, control Western blots illustrating the presence of endogenous syntenin and CD9 signals. Ponceau red staining served as a loading and transfer control. **(c)** Graph showing the average luminescence signals (RLU, Y-axis), + SEM (SE for CD63), obtained after various dilutions of CCM sEVs containing different constructs as indicated. Signals were obtained after incubation with Furimazine in the presence of 0.05% Triton X-100 and 2.5 µg rLgBiT. See Supplementary Figs. 3b and 3c for set-up assays. The dashed line indicates the dilution selected for total CCM sEV dose measurements in further experiments. The n-number indicates the number of independent biological repeats. **(d)** Schematic representation showing the experimental setup to verify the intraluminal location of HiBiT-tagged constructs (illustrated for syntenin). HiBiT and LgBiT can reconstitute into an enzymatically active form when not separated by a membrane. To determine the internal/external orientation of HiBiT-tagged syntenin, CCM sEVs were incubated with rLgBiT in the presence or absence of Triton X-100, followed by Furimazine substrate addition (not shown) and luminescence measurement. The n-number indicates the number of independent biological repeats. **(e)** Bar graph showing average luminescence signals (relative light units, RLU, Y-axis) + SEM obtained from CCM sEVs containing HiBiT-syntenin, HiBiT-CD63, or NL-syntenin (used as positive control). CCM sEVs were treated or not with Triton X-100 and/or rLgBiT, as indicated at the bottom. The membrane-permeant substrate, Furimazine was used throughout. Note that luminescence signal for HiBiT-fusions was detected only upon membrane permeabilization and rLgBiT addition, indicating intraluminal localization of the HiBiT

696 tag. As expected, NL-syntenin luminescence signal was unaffected by the presence of
697 Triton X-100 and/or rLgBiT. Each point represents an independent biological replicate.
698 One-way ANOVA with Tukey's correction for multiple comparisons (HiBiT data only)
699 was applied. Related to **Supplementary Fig. 4**.

700 **Figure 3. Capture versus internalization of sEV NL-syntenin and measurements**
701 **of sEV HiBiT-syntenin full dose, internalization and delivery to the cytosol of**
702 **recipient cells by NL complementation assay. (a)** Average luminescence signals
703 (relative light units, RLU, Y-axis) + SEM obtained from MCF-7 WT cells after incubation
704 at 37°C, for different periods of time, with CCM sEVs (30p/r) containing NL-syntenin.
705 After incubation, cells were trypsinized or not, as indicated. Signals measured after
706 washing (in the absence of trypsin) were taken as a measure of sEV capture together
707 with internalization, whereas signals measured after trypsinization and washing were
708 taken as a measure of sEV internalization only. The luminescence signals were
709 measured after addition of the membrane-permeant substrate Furimazine. Note, that
710 capture increases continuously over time, whereas the internalization fraction rapidly
711 reaches a plateau value. The n-number indicates the number of independent biological
712 repeats. **(b)** Schematic overview recapitulating the different measurements (left) and
713 the experimental approach (right). Briefly, for the determination of the full dose (i), an
714 aliquot of the CCM sEVs was incubated with rLgBiT in the presence of Triton X-100
715 before Furimazine addition. For the determination of the internalization (ii) and the
716 cytosolic delivery (iii), MCF-7 LgBiT were incubated with CCM sEVs (30p/r) for 4 hours,
717 washed and trypsinized. Samples were split in two equal fractions. The first fraction
718 was incubated with Triton X-100, rLgBiT before Furimazine addition to measure the
719 internalized sEVs. The second fraction was solely incubated with Furimazine to
720 measure the sEV cytosolic delivery. **(c)** Bars and whiskers graphs showing the median
721 luminescence signals with minimal and maximal values, obtained with CCM sEVs
722 containing HiBiT-syntenin (left) or NL-syntenin used as positive control (right).
723 Background signals from MCF-7 LgBiT cells treated with Mock CCM sEVs were
724 subtracted. Each CCM sEV preparation served for 2-3 independent measurements of
725 internalization and cytosolic delivery with at least 2 technical repeats. Related to
726 **Supplementary Fig. 5.**

727 **Figure 4. Mapping of syntenin molecular determinants involved in cytosolic**
728 **delivery. (a)** Schematic representation of syntenin protein. The N-terminal domain is

729 in grey, PDZ domains are in blue, and C-terminal domain is in white. The wild-type form
730 (upper scheme) and the various mutants tested in this study are represented. **(b)** Bars
731 and whiskers graphs showing the median luminescence signals with minimal and
732 maximal values, obtained with CCM sEVs containing HiBiT-syntenin WT or different
733 HiBiT-syntenin mutants as indicated. Background signals from MCF-7 LgBiT cells
734 treated with Mock CCM sEVs were subtracted. Three to 15 different preparations of
735 syntenin WT or mutant CCM sEVs were used (Supplementary Fig. 6b) to collect 6-39
736 independent measurements, as indicated. One-way ANOVA with Dunnet's correction
737 for multiple comparisons was applied, comparing WT syntenin cytosolic signal with that
738 of the mutants. Each CCM sEV preparation (see Supplementary Fig. 6b) served for 1-
739 3 independent measurements of cytosolic delivery. Related to **Supplementary Fig. 6.**